

The non-thermal emission of extended radio galaxy lobes with curved electron spectra

Peter Duffy¹ and Katherine M. Blundell²

¹*UCD School of Physics, University College Dublin, Dublin 4, Ireland*

²*University of Oxford, Astrophysics, Keble Road, Oxford, OX1 3RH, U.K.*

31 May 2021

ABSTRACT

The existing theoretical framework for the energies stored in the synchrotron-emitting lobes of radio galaxies and quasars doesn't properly account for the curved spectral shape that many of them exhibit. We characterise these spectra using parameters that are straightforwardly observable in the era of high-resolution, low-frequency radio astronomy: the spectral curvature and the turnover in the frequency spectrum. This characterisation gives the Lorentz factor at the turnover in the energy distribution (we point out that this is distinctly different from the Lorentz factor corresponding to the turnover frequency in a way that depends on the amount of curvature in the spectrum) and readily gives the equipartition magnetic field strength and the total energy of the radiating plasma obviating the need for any assumed values of the cutoff frequencies to calculate these important physical quantities. This framework readily yields the form of the X-ray emission due to inverse-Compton (IC) scattering of Cosmic Microwave Background (CMB) photons by the electrons in the plasma having Lorentz factors of ~ 1000 . We also present the contribution to CMB anisotropies due to relativistic plasmas such as giant radio galaxy lobes, expressed in terms of the extent to which the lobes have their magnetic field and particle energies are in equipartition with one another.

Key words: Galaxies: Jets, Radio galaxies

1 INTRODUCTION

In order to quantify the feedback and influence of the jets and lobes of radio galaxies and quasars in terms of the energy and heat they inject into their environments (hence their influence on cosmic structure formation) and also their contamination to primordial anisotropies in the Cosmic Microwave Background (CMB) it is necessary to understand the nature of the underlying particle energy spectrum of these plasmas. For example, to calculate the energy stored in radio galaxy lobes, it is necessary to integrate over the entire energy distribution of the particles in the plasma which constitutes the lobes. Traditionally, this is calculated by assuming that these plasmas have very simple power-law energy distributions (e.g. Longair 1981; Miley 1980) but there are two distinct drawbacks of this approach: the first problem is that radio spectra are frequently observed to be curved rather than power-law (e.g. Laing & Peacock 1980; Landau et al 1986; Carilli et al 1991; Blundell, Rawlings & Willott 1999; Klamer et al. 2006; Jamrozy et al. 2008). The second problem is that the lower limit of the power-law approximation of this distribution of energies (expressed in terms of

Lorentz factor γ), also known as the low-energy cutoff or turnover, referred to as γ_{\min} has been unconstrained for decades (e.g. $\gamma_{\min} = 1$ is used by Hardcastle (2005) and also by Kaiser et al. (1997), $\gamma_{\min} = 10$ is used by Croston et al (2005), $\gamma_{\min} = 100$ is used by Carilli et al (1991), 1000 is taken by Wardle et al (1998)); uncertainty on this scale of the low-energy cutoff leads to orders of magnitude uncertainty in the estimate of the energy stored by the plasma reservoirs (Mocz et al. 2011).

We present a new formalism which overcomes the difficulties previously encountered in inferring energies and magnetic fields from synchrotron-emitting plasma exhibiting curved spectra, characterising this curved spectral shape with curvature coefficients that are straightforwardly fitted in terms of the observed peak frequency (ν_{peak}) and the observed curvature (q) giving simple expressions for the magnetic field strength (B) and the total energy density (e). We demonstrate consistency with the traditional power-law case in the appropriate limit. We present a specific discussion of how the magnetic field itself can be determined if equipartition is assumed and quantify the extent to which these plasma lobes are contaminants of primordial CMB

anisotropies on the relevant angular scales, noting that this extent is a strong function of whether the plasma lobes have their magnetic field and particle energies in equipartition.

2 THE CURVED SPECTRA OF CLASSICAL DOUBLE RADIO SOURCES

Blundell, Rawlings & Willott (1999) found for the complete samples of low-frequency selected classical double radio galaxies they analysed across a wide range of frequencies that $\sim 70\%$ of these objects have curved synchrotron spectra at radio wavelengths. They fitted these spectra of frequency ν and emissivity L_ν to functions of the following form:

$$\ln(L_\nu) = a_0 + a_1 \ln(\nu) + a_2 [\ln(\nu)]^2. \quad (1)$$

The consistently curving spectra of such sources have historically been neglected when their energies and magnetic field strengths have been estimated via the Longair (1981) and Miley (1980) formalism. Often it has been assumed that curvature is simply a high-energy phenomenon only arising from synchrotron ageing in the GHz regime. However, there are no definitive examples of a power-law spectrum being observed at low radio frequencies with bolt-on curvature (such as that from synchrotron ageing) only being observed at higher radio frequencies. Indeed, Blundell & Rawlings (2000) explained why the origin of a curved spectrum cannot be attributed to the ageing of a synchrotron spectrum and so the paradigm of an intrinsically curved electron-energy spectrum $N(\gamma)$ cannot be dismissed. Studies of complete samples of classical double radio sources showed that the dominant energy-loss mechanism for radio lobes are not synchrotron losses but adiabatic expansion losses (Blundell, Rawlings & Willott 1999) which are energy-independent (Scheuer & Williams 1968). It is most interesting in this regard that Rudnick et al. (1994), in a detailed analysis of the spatially resolved spectral shape of the famous classical double radio galaxy Cygnus A, found *no evidence for any variation in the curvature of $N(\gamma)$ throughout even the oldest or youngest regions of this prototypical object*. This points to an intrinsically curved particle spectrum in the plasma lobes of Cygnus A.

We briefly review and reject three possibilities of this spectral curvature being caused by external factors, rather than arising from the inherent particle distribution: (i) Free-free absorption: in principle, free-free absorption of synchrotron photons by the medium surrounding the radio lobes could cause spectral curvature. However, since many radio galaxy and quasar lobes have lengths of 100s of kpc (e.g. Blundell, Rawlings & Willott 1999) which lie way beyond their host galaxies, this explanation can be dismissed as a dominant effect except for the innermost 10s of kpc of which might have sufficient gas densities for this absorption to be significant. (ii) Synchrotron self-absorption: if the plasma is optically thick to synchrotron photons, as may be the case at very low radio frequencies, then this could dramatically curve the spectra. However, this would produce rising spectra not falling spectra characterised by the sources whose spectra we focus on in this paper. (iii) The Razin effect might in principle choke off synchrotron radiation, if the plasma particle density were sufficiently high, but simple estimates suggest that this would require particle densities

of 10^{16} m^{-3} which is orders of magnitude higher than believed to be the case in lobes or even hotspots. Thus it is reasonable to assume that in the vast majority of cases the observed curvature of frequency spectra arises because of an intrinsically curved particle spectrum rather than because of external attenuating influences.

2.1 The particle spectrum

Curved synchrotron spectra described in equation 1 suggest an underlying energetic electron distribution with the shape

$$\ln(N(\gamma)) = \ln(N_0) - p \ln(\gamma) - q(\ln(\gamma))^2 \quad (2)$$

where $N(\gamma)$ is the differential number of electrons per unit volume with Lorentz factor γ and N_0 is the amplitude of that spectrum extrapolated down to $\gamma = 1$. The curvature of the spectrum is contained in the *curvature index* q , while the traditional power-law limit, with index p , is recovered when $q = 0$. We note that when $q > 0$, giving a local maximum to the spectrum, that the index p (which is the slope of the distribution extrapolated to $\gamma = 1$) must be negative. While curved spectra can also contain low and high energy cutoffs, these are less critical than in the pure power-law case where the energy density is dominated by one of these cutoffs which are invariably outside the observational window. In the curved case the energy density, total luminosity and other physically important quantities are determined by the local maximum in the energy spectrum at γ_{peak} . The synchrotron energy-loss rate for an electron with Lorentz factor γ in a magnetic field B is given by

$$\dot{E} = -\frac{4}{3} \sigma_T c \gamma^2 \frac{B^2}{2\mu_0} = -b_0 \gamma^2 B^2 \quad (3)$$

where σ_T is the Thomson cross section and $b_0 = 1.0588 \times 10^{-14} \text{ WHz}^{-1} \text{ T}^{-2}$. While a single particle will radiate across a range of frequencies, we use here the well-known approximation that all of the emission is radiated at the single frequency given by:

$$\nu = \gamma^2 \frac{eB}{2\pi m_e} = b_1 \gamma^2 B \quad (4)$$

with $b_1 = 2.799 \times 10^{10} \text{ Hz T}^{-1}$. The differential energy emitted per unit volume at frequency ν by a spectrum of energetic particles with differential energy spectrum per unit volume $N(E)$ is then given by

$$L_\nu d\nu = -\dot{E} N(E) dE = -\dot{E} N(\gamma) d\gamma \quad (5)$$

so that

$$L_\nu = \frac{b_0}{2b_1} B \left(\frac{\nu}{b_1 B} \right)^{1/2} N \left(\left(\frac{\nu}{b_1 B} \right)^{1/2} \right). \quad (6)$$

Inserting the quadratically-curved particle spectrum of equation 2, we obtain the required synchrotron spectrum in the form

$$\ln(L_\nu) = a_0 - \left(\frac{p-1}{2} \right) \ln(\hat{\nu}) - \frac{q}{4} (\ln(\hat{\nu}))^2 \quad (7)$$

with $\hat{\nu} = \nu/b_1 B$ and where the constant a_0 depends on the magnetic field strength. We can now relate the coefficients of the synchrotron spectrum in equation 1 to those of the particle spectrum: $a_1 = -(p-1)/2$ and $a_2 = -q/4$.

A more useful expression for the curved particle distribution replaces the parameters N_0 and p in favour of the

position, γ_{peak} , and differential number density $N_{\text{peak}} \equiv N(\gamma_{\text{peak}})$ at the local maximum. The energy-dependent slope of the distribution is

$$\frac{d \ln N}{d \ln \gamma} = -p - 2q \ln(\gamma) \quad (8)$$

so that the differential number of particles has a maximum value at

$$\gamma_{\text{peak}} = \exp\left(-\frac{p}{2q}\right). \quad (9)$$

Since $q > 0$ the parameter p must be negative for the spectra characteristically exhibited by radio galaxies and quasars so that a spectrum with a local maximum at $\gamma_{\text{peak}} > 1$ must be rising at the point where $\gamma = 1$. The electron distribution can be written in terms of the position and height of the spectral peak and the curvature index:

$$\ln(N) = \ln(N_{\text{peak}}) - q (\ln(\gamma) - \ln(\gamma_{\text{peak}}))^2 \quad (10)$$

which we can more easily relate to the frequency and intensity of the maximum synchrotron luminosity. The particle spectrum is then

$$N(\gamma) = N_{\text{peak}} \exp\left[-q \left(\ln\left(\frac{\gamma}{\gamma_{\text{peak}}}\right)\right)^2\right]. \quad (11)$$

Power-law spectra in radio lobes have traditionally been characterised by a lower cutoff, γ_{min} , the value of the spectrum at that point, N_{min} , and the index p . In the curved case we also have three parameters; the position of the peak, γ_{peak} , the value of the distribution at that Lorentz factor, N_{peak} , and the curvature index q . The number and energy densities of the curved distribution are:

$$n = \int N(\gamma) d\gamma \quad \text{and} \quad U_{\text{P}} = \int \gamma m_e c^2 N(\gamma) d\gamma \quad (12)$$

which will depend on γ_{peak} , N_{peak} and q , with a very weak dependence on any low-energy cutoff. Calculating moments of a quadratic distribution (on the *log-log* plane) is non-trivial. However, it can be shown (see Appendix) that the spectrum described in equation 11 also has the shape of a *log-normal* distribution, which is the probability distribution for the exponent of a random variable with a Gaussian distribution. The moments of *log-normal* distributions are well known and allow us to derive expressions for the number density and energy density in terms of peak properties (γ_{peak} and N_{peak}) and spectral curvature (q), as follows:

$$n = \sqrt{\frac{\pi}{q}} e^{1/4q} \gamma_{\text{peak}} N_{\text{peak}} \quad (13)$$

and

$$U_{\text{P}} = \sqrt{\frac{\pi}{q}} e^{1/4q} \gamma_{\text{peak}}^2 m_e c^2 N_{\text{peak}} = n m_e c^2 e^{3/4q} \gamma_{\text{peak}}. \quad (14)$$

Frequency-resolved observations of a synchrotron spectrum will allow us to calculate q directly but, without knowledge of the magnetic field, we cannot directly infer values for γ_{peak} and N_{peak} unambiguously from the peak emission. Relating the peak of the energy spectrum to the frequency, and intensity, of the maximum emission depends not only on B but also on the spectral curvature as we now show.

2.2 The synchrotron spectrum

The underlying electron distribution will, in the presence of a magnetic field, give rise to synchrotron emission with a local maximum at frequency ν_{max} where the differential number density will determine the value of the emissivity at this frequency which we term $L_{\nu_{\text{max}}}$. Since the curvature of the synchrotron spectrum is $q/4$ it can be shown, in an analogous way to equation 10, that the frequency spectrum can be written in the form:

$$\ln(L_{\nu}) = \ln(L_{\nu_{\text{max}}}) - \frac{q}{4} (\ln(\nu) - \ln(\nu_{\text{max}}))^2. \quad (15)$$

It is tempting to assume that electrons with a Lorentz factor of γ_{peak} give rise to the emission at ν_{max} , but this is not the case as Fig 1 illustrates. The emissivity of a single particle scales with γ^2 so that particles which are slightly more energetic than those at γ_{peak} , although fewer in number, will radiate more intensely. This is most easily seen by returning to the approximation where an electron with a Lorentz factor γ emits at a single frequency $\nu \propto \gamma^2$ so that

$$L_{\nu} \propto \dot{E}(\gamma) N(\gamma) \frac{d\gamma}{d\nu} \propto \gamma^2 N(\gamma) \nu^{-1/2} \propto \gamma N(\gamma), \quad (16)$$

and the emission is at its most intense not for the Lorentz factor that maximises $N(\gamma)$ (i.e. γ_{peak}) but rather for the value that maximises $\gamma N(\gamma)$ which is found from

$$\frac{d \ln(\gamma N)}{d \ln \gamma} = 1 - p - 2q \ln(\gamma). \quad (17)$$

Thus, the particles responsible for the maximum emission in the frequency spectrum are shifted upwards in energy from the particles at the peak of the energy distribution, and have a Lorentz factor given by

$$\gamma(\nu_{\text{max}}) = \gamma_{\text{peak}} e^{1/2q}. \quad (18)$$

Figure 1 illustrates the effect of curvature for a range of values between $q = 0.01$ and $q = 5$. For example, when $q = 0.2$ there is more than an order of magnitude difference between the energies of electrons at the peak of distribution and those electrons that give rise to the most intense synchrotron emission. We can now relate ν_{max} and $L_{\nu_{\text{max}}}$ to the corresponding parameters for the electron distribution, γ_{peak} and N_{peak} as follows:

$$\nu_{\text{max}} = b_1 \gamma(\nu_{\text{max}})^2 B = b_1 e^{1/q} \gamma_{\text{peak}}^2 B \quad (19)$$

$$\begin{aligned} L_{\nu_{\text{max}}} &= \frac{b_0}{2b_1} B \gamma(\nu_{\text{max}}) N(\gamma(\nu_{\text{max}})) \\ &= \frac{b_0}{2b_1} e^{1/4q} B \gamma_{\text{peak}} N_{\text{peak}}. \end{aligned} \quad (20)$$

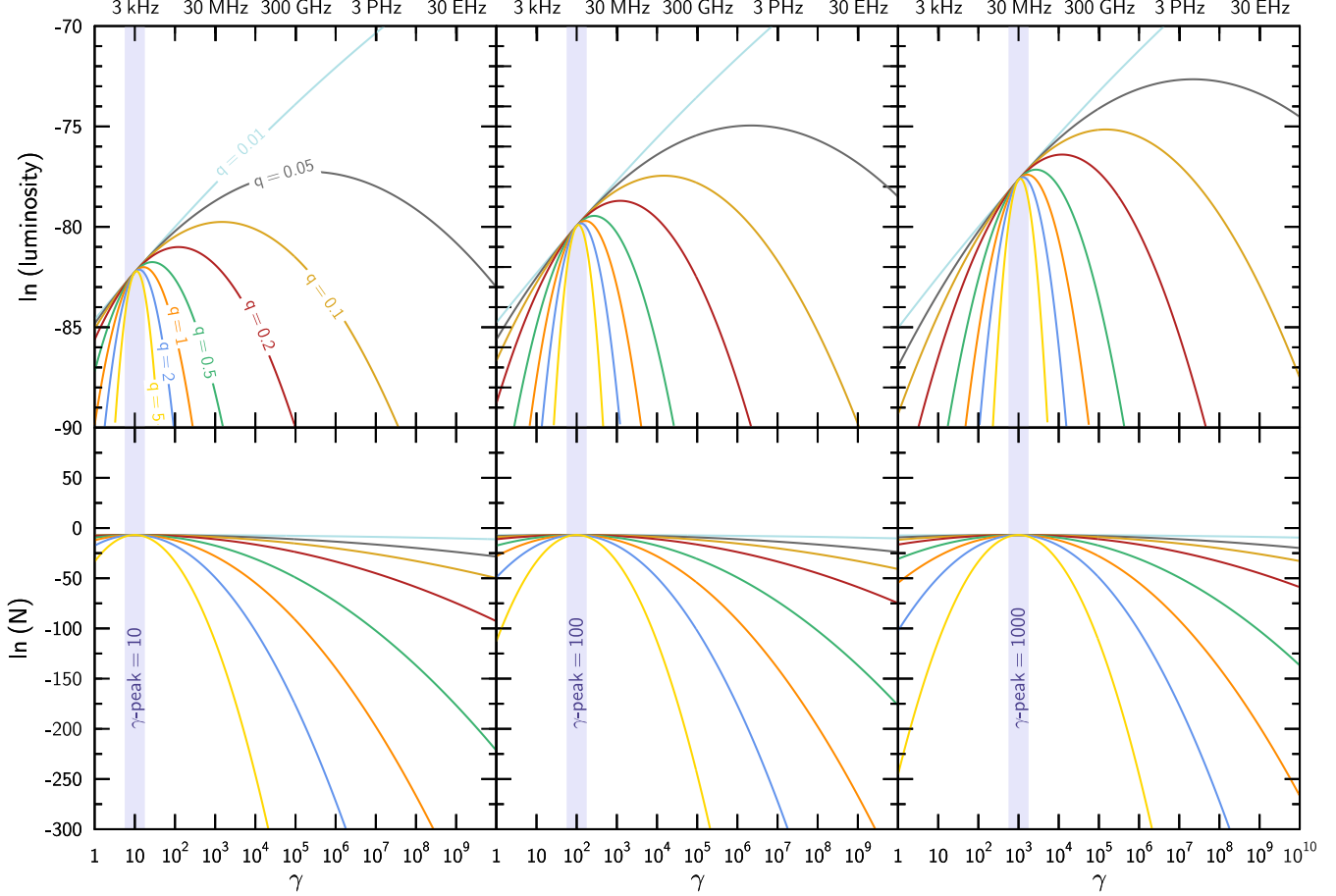


Figure 1. This figure illustrates how for different values of q the energies of the electrons at the peak of the particle energy distribution are distinctly different from those electrons that give rise to the most intense synchrotron emission in the frequency spectrum.

2.3 Equipartition magnetic field strength

We can express γ_{peak} , N_{peak} , n (measured in m^{-3}) and U_{P} (J/m^3) in terms of the observable quantities ν_{max} , $L_{\nu_{\text{max}}}$ and q , subject to the uncertainty in the magnetic field

$$\gamma_{\text{peak}} = \frac{e^{-1/2q}}{\sqrt{b_1}} \nu_{\text{max}}^{1/2} B^{-1/2} = 5.98 \times 10^3 e^{-1/2q} \left(\frac{\nu_{\text{max}}}{1 \text{ GHz}} \right)^{1/2} \left(\frac{B}{1 \text{ nT}} \right)^{-1/2} \quad (21)$$

$$N_{\text{peak}} = \frac{2b_1^{3/2}}{b_0} e^{1/4q} L_{\nu_{\text{max}}} \nu_{\text{max}}^{-1/2} B^{-1/2} = 8.85 \times 10^{-6} e^{1/4q} \left(\frac{L_{\nu_{\text{max}}}}{10^{-35} \text{ W m}^{-3} \text{ Hz}^{-1}} \right) \left(\frac{\nu_{\text{max}}}{1 \text{ GHz}} \right)^{-1/2} \left(\frac{B}{1 \text{ nT}} \right)^{-1/2} \quad (22)$$

$$n = \frac{2b_1}{b_0} \sqrt{\frac{\pi}{q}} L_{\nu_{\text{max}}} B^{-1} = 5.29 \times 10^{-2} \sqrt{\frac{\pi}{q}} \left(\frac{L_{\nu_{\text{max}}}}{10^{-35} \text{ W m}^{-3} \text{ Hz}^{-1}} \right) \left(\frac{B}{1 \text{ nT}} \right)^{-1} \quad (23)$$

$$U_{\text{P}} = \frac{2\sqrt{b_1}}{b_0} m_e c^2 \sqrt{\frac{\pi}{q}} e^{1/4q} L_{\nu_{\text{max}}} \nu_{\text{max}}^{1/2} B^{-3/2} = 2.59 \times 10^{-11} \sqrt{\frac{\pi}{q}} e^{1/4q} \left(\frac{L_{\nu_{\text{max}}}}{10^{-35} \text{ W m}^{-3} \text{ Hz}^{-1}} \right) \left(\frac{\nu_{\text{max}}}{1 \text{ GHz}} \right)^{1/2} \left(\frac{B}{1 \text{ nT}} \right)^{-3/2} \quad (24)$$

The ratio of particle to magnetic energy density is then

$$\theta \equiv \frac{U_{\text{P}}}{U_{\text{B}}} = 65.08 \sqrt{\frac{\pi}{q}} e^{1/4q} \left(\frac{L_{\nu_{\text{max}}}}{10^{-35} \text{ W m}^{-3} \text{ Hz}^{-1}} \right) \left(\frac{\nu_{\text{max}}}{1 \text{ GHz}} \right)^{1/2} \left(\frac{B}{1 \text{ nT}} \right)^{-7/2} \quad (25)$$

The magnetic field strength in equipartition with the energetic electrons is then (with $q_{0.2} \equiv q/0.2$)

$$B_{\text{equip}} = 2.01 \left(\frac{e^{1/2q}}{q} \nu_{\text{max}} L_{\nu_{\text{max}}}^2 \right)^{1/7} = 6.98 \left(\frac{e^{1/2q_{0.2}}}{q_{0.2}} \right)^{1/7} \left(\frac{\nu_{\text{max}}}{1 \text{ GHz}} \right)^{1/7} \left(\frac{L_{\nu_{\text{max}}}}{10^{-35} \text{ W m}^{-3} \text{ Hz}^{-1}} \right)^{2/7} \text{ (nT)} \quad (26)$$

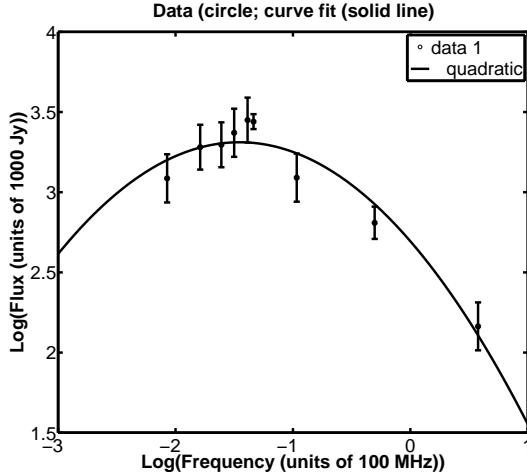


Figure 2. Plot of the radio frequency spectrum of the prototypical powerful classical double radio galaxy Cygnus A and the best quadratic fit to these points.

where B_{equip} is here expressed in nano-Tesla. Therefore if we can be confident that the magnetic field energy of a plasma is in equipartition with its particle energy then we have obtained B -field measuring machinery in terms of the observables ν_{max} , $L_{\nu_{\text{max}}}$ and q .

The magnetic field that minimises the total energy, B_{min} , can be obtained from the expression for the total electron and magnetic field energy densities

$$U = U_{\text{P}} + U_{\text{B}} = \frac{c_1}{B^{3/2}} + c_2 B^2$$

where c_1 and c_2 are constants such that $B_{\text{equip}} = (c_1/c_2)^{2/7}$. The energy density is a minimum for $B_{\text{min}} = (3c_1/4c_2)^{2/7} = 0.92B_{\text{equip}}$ so that, as in the power law case, the equipartition and minimum energy B fields are comparable.

2.4 Cygnus A

We now apply these results to the lobes of the prototypical classical double radio galaxy, Cygnus A. In Figure 2 we show both the observed spectra and best-fit quadratic, on the \log - \log plane. The equation for the best-fit curve is

$$y = -0.29x^2 - 0.85x + 2.7 \quad (27)$$

where

$$y \equiv \ln\left(\frac{F_\nu}{10^3 \text{ Jy}}\right) \quad \text{and} \quad x \equiv \ln\left(\frac{\nu}{100 \text{ MHz}}\right). \quad (28)$$

The relation between emissivity and frequency determines q through the quadratic term,

$$\ln(L_\nu) = -\frac{q}{4}(\ln \nu)^2 + \dots \quad (29)$$

Converting from flux density (F_ν) to emissivity (L_ν) (which involves the distance to the source and its volume) and normalising the frequency to arbitrary units will not change the coefficient of the quadratic term. Therefore, for Cygnus A we have

$$\frac{q}{4} = 0.29 \Rightarrow q = 1.16 \quad (30)$$

and the emission has a maximum at

$$\nu_{\text{max}} = 23 \text{ MHz} \quad \text{with} \quad F_{\nu_{\text{max}}} = 2.77 \times 10^4 \text{ Jy}. \quad (31)$$

Since the source is at a distance of $D = 600 \text{ Mlyr}$ and has a volume estimated to be $V \approx 1.73 \times 10^{63} \text{ m}^3$, the peak emissivity is

$$L_{\nu_{\text{max}}} = 6.52 \times 10^{-35} \text{ Wm}^{-3} \text{ Hz}^{-1}. \quad (32)$$

Using equations 21, 22, 23 and 24 we can express γ_{peak} , N_{peak} , n and e for Cygnus A in terms of the magnetic field B_{nT} (in units of 1 nT),

$$\gamma_{\text{peak}} = 5.91 \times 10^2 B_{\text{nT}}^{-1/2} \quad (33)$$

$$N_{\text{peak}} = 4.71 \times 10^{-4} B_{\text{nT}}^{-1/2} \quad (34)$$

$$n = 0.57 B_{\text{nT}}^{-1} \quad (35)$$

$$U_{\text{P}} = 5.21 \times 10^{-11} B_{\text{nT}}^{-3/2}. \quad (36)$$

The equipartition field is then $B_{\text{nT}} = 4$ implying a peak to the electron distribution at $\gamma_{\text{peak}} = 296$, a number density of $n = 0.14 \text{ m}^{-3}$ and an energy density of $U_{\text{P}} = 6.37 \times 10^{-12} \text{ Jm}^{-3} \approx 40 \text{ eV cm}^{-3}$.

However, there is compelling evidence from multiwavelength observations of Cygnus A (Steenbrugge et al. 2008) that a peak in the electron distribution along the jet must be above a few times 10^3 in Lorentz factor. Taking $\gamma_{\text{peak}} = 10^4$ we can invert the above argument to give $B_{\text{nT}} \approx 3.49 \times 10^{-3}$, which is well below equipartition. In this case we have a weak field, peaked at a high Lorentz factor, and with a high number density of energetic electrons, $n \approx 160 \text{ m}^{-3}$. The existence of a high number density of particles at $\gamma_{\text{peak}} = 10^4$ has important implications for the relativistic Sunyaev-Zeldovich effect from this source, as will be shown in the next section.

3 CURVED ELECTRON SPECTRA AND THE CMB

In addition to their acceleration in the background magnetic field the relativistic electrons will also interact with the CMB. Two interesting, and potentially observable, effects can then arise. First, Inverse Compton scattering off the CMB (ICCMB) will result in X-ray emission (for $\gamma_{\text{peak}} \sim 10^3$). This spectrum will be peaked at a frequency determined by γ_{peak} , q and the frequency at which the maximum intensity occurs in the CMB spectrum. Second, photons in the Rayleigh-Jeans regime of the CMB will be upscattered by the energetic electrons leading to an observed reduction in the CMB temperature: the Sunyaev Zeldovitch (SZ) effect. We examine each of these below.

An energetic electron in a photon field with energy density U_{rad} will lose energy through Inverse-Compton scattering at the rate,

$$\dot{E} = -\frac{4}{3} \sigma_{\text{T}} c \gamma^2 U_{\text{rad}}. \quad (37)$$

The electrons scatter the ambient CMB photons producing higher energy photons (of frequency ν_{X}) according to:

$$\frac{\nu_X}{\nu_{\text{CMB}}} = \left(\frac{4}{3}\right) \gamma^2 - \frac{1}{3} \approx \frac{4}{3} \gamma^2. \quad (38)$$

As in the synchrotron case, the maximum intensity X-ray emission will not correspond to ICCMB scattering off γ_{peak} particles but rather particles with a Lorentz factor of $\gamma(\nu_{\text{max}}) = \gamma_{\text{peak}} e^{1/2q}$; i.e. the maximum intensities in both the radio synchrotron and ICCMB emission are caused by particles of the same Lorentz factor (the one for which $\gamma N(\gamma)$ is a maximum). This occurs because the dependence of E and the dominant synchrotron emission frequency have the same dependence on γ . Hence, the ratio of the peak emission in synchrotron to that in X-rays will only depend on the ratio of magnetic field energy density to the equivalent energy density in the CMB (as in the power-law case). Moreover, if we were to observe a maximum in the ICCMB spectrum at $\nu_{\text{IC,max}}$ then we can relate that to the shape of the particle distribution (for $q \neq 0$) through

$$\nu_{\text{IC,max}} \approx \frac{4}{3} \gamma_{\text{peak}}^2 e^{1/q} \nu_{\text{CMB}}. \quad (39)$$

With $\gamma_{\text{peak}} = 10^3$ and $q = 0.2$, a source at redshift z would then have an ICCMB spectrum peaked at

$$\frac{h\nu_{\text{IC,max}}}{1 \text{ keV}} \approx 130(1+z) \left(\frac{\gamma_{\text{peak}}}{10^3}\right)^2 e^{1/q_{0.2}} \quad (40)$$

in the hard X-ray to soft gamma-ray region. It is useful to compare this prediction with that of Blundell et al. (2006) who consider the ICCMB spectrum from a giant radio galaxy at redshift $z \sim 2$ where the electron spectrum is a power law with a low-energy cutoff at $\gamma_{\text{min}} \gg 1$. When the index $p > 2$, the differential number and energy densities are dominated by particles at this low energy cutoff. The X-ray ICCMB emission will therefore peak at a frequency of $\nu_{\text{X,min}} \approx \gamma_{\text{min}}^2 \nu_{\text{CMB}}$, with the emission falling off rapidly for lower frequencies and with a power law above $\nu_{\text{X,min}}$. But in the curved case, just as with synchrotron emission, it is particles with a Lorentz factor of $\gamma_{\text{peak}} e^{1/2q}$ that will give rise to the most intense ICCMB emission. Since the emitted frequency scales quadratically with γ this can have a dramatic effect on $\nu_{\text{IC,max}}$. For $\gamma_{\text{peak}} = 10^3$ and $q = 0.2$ this pushes the peak emission into the hard X-ray to soft gamma-ray region. For a low-energy power-law cutoff at $\gamma_{\text{min}} = 10^3$ (and with $p > 2$) the ICCMB emission peaks at frequencies of about a few keV — some two orders of magnitude below a curved spectrum with $\gamma_{\text{peak}} = 10^3$ and $q = 0.2$. While the position of the peak can be quite different, depending on q , for curved and power-law spectra with $\gamma_{\text{peak}} = \gamma_{\text{min}}$, the intensity of the emission will, of course, depend in each case on the number density of energetic particles.

The SZ effect predicts a reduction (for the Rayleigh-Jeans regime) in the temperature of the CMB for the (optically thin) scattering of photons through a hot electron gas in a galaxy cluster. When the CMB photons are scattered by relativistic, as opposed to thermal, particles the temperature is also reduced (Birkinshaw et al 1999; McKinnon, Owen & Eilek 1991) and is related to the optical depth, τ , by

$$\frac{\Delta T}{T} \approx -\tau \quad (41)$$

where

$$\tau = 2\sigma_T n R_{\text{lobe}}, \quad (42)$$

where R_{lobe} is the path length through the plasma lobe. Our number density of target electrons is no longer a thermal distribution but non-thermal and curved so that

$$n = \sqrt{\frac{\pi}{q}} e^{1/4q} \gamma_{\text{peak}} N_{\text{peak}}. \quad (43)$$

We would therefore expect a reduction of the CMB temperature in the direction of a lobe of the order

$$\frac{\Delta T}{T} \approx -2\sigma_T n R_{\text{lobe}} \approx -2\sqrt{\frac{\pi}{q}} e^{1/4q} \gamma_{\text{peak}} N_{\text{peak}} \sigma_T R_{\text{lobe}}. \quad (44)$$

From equations 21 and 22, $\gamma_{\text{peak}} N_{\text{peak}}$ depends on the peak synchrotron emissivity, magnetic field strength and index q

$$\gamma_{\text{peak}} N_{\text{peak}} = 5.29 \times 10^{-2} e^{-1/4q} \left(\frac{L_{\nu_{\text{max}}}}{10^{-35} \text{ W m}^{-3} \text{ Hz}^{-1}}\right) \left(\frac{B}{1 \text{ nT}}\right)^{-1}. \quad (45)$$

The relativistic SZ effect gives a decrease in temperature that can be related to the observable peak and curvature of the synchrotron spectrum, and the magnetic field strength. For a lobe with a scale $R = 10 \text{ kpc}$ we get

$$\frac{\Delta T}{T} \approx \frac{3.85 \times 10^{-9}}{\sqrt{q}} \left(\frac{R_{\text{lobe}}}{10 \text{ kpc}}\right) \left(\frac{L_{\nu_{\text{max}}}}{10^{-35} \text{ W m}^{-3} \text{ Hz}^{-1}}\right) \left(\frac{B}{1 \text{ nT}}\right)^{-1} \quad (46)$$

giving a temperature reduction of a few nK for Cygnus A if the magnetic field is in equipartition and of the order of several nT.

However, in the previous section it was argued that Cygnus A might contain a high density of particles at $\gamma_{\text{peak}} = 10^4$ in order to explain the synchrotron emission in a magnetic field that is well below equipartition, $B_{\text{nT}} = 3.46 \times 10^{-4}$. A high density of ultrarelativistic particles in a such a weak field gives a fractional reduction in the CMB temperature of

$$\frac{\Delta T}{T} \approx 6.69 \times 10^{-5} \left(\frac{R_{\text{lobe}}}{10 \text{ kpc}}\right). \quad (47)$$

which is at a level that is detectable by current technology.

4 SUMMARY

We have presented a formalism which gives the easy derivation of important physical quantities of plasma lobes (energy, magnetic field strength, optical depth hence fraction of CMB upscattered) from the simple characterisation of their spectra as quadratic on the log-frequency log-luminosity plane. We also point out that the peak of the curved distribution of particles' Lorentz factors in a plasma lobe will not map directly to the frequency at which the peak intensity is observed — this is true for both the synchrotron emission, and the ICCMB scattered emission observed in the X-rays or higher energies. We have also quantified the contribution to CMB anisotropies from such relativistic plasma lobes as a function of the extent to which such plasma lobes exhibit equipartition of energies stored in particles and magnetic fields.

ACKNOWLEDGMENTS

The authors are grateful for the support of Science Foundation Ireland, the Research Centre of St John's College

Oxford, the Royal Irish Academy and the Royal Society. KMB thanks the Royal Society for a University Research Fellowship. PD acknowledges support from Science Foundation Ireland under grant 05/RFP/PHY0055.

REFERENCES

- Aitchison, J. & Brown J.A.C. 1957, CUP
 Birkinshaw, M., 1999 Phys. Rep., 310, 97
 Blundell, K. M., Fabian, A. C., Crawford, C. S., Erlund, M. C., & Celotti, A. 2006, ApJ Lett, 644, L13
 Blundell, K. M., Rawlings, S. & Willott, C. J, 1999, AJ, 117, 677
 Blundell, K. M. & Rawlings, S., 2000, AJ, 119, 1111
 Carilli, C. L., Perley, R. A., Dreher, J. W. & Leahy, J. P., 1991, AJ, 383, 554
 Celotti, A., Kuncic, Z., Rees, M. J. & Wardle, J. F. C., 1998, MNRAS, 293, 288
 Celotti, A., 2003, Ap&SS, 288, 175
 Croston, J. H., Hardcastle, M. J., Harris, D. E., Belsole, E., Birkinshaw, M. & Worrall, D. M., 2005, ApJ, 626, 733
 Erlund, M. C., Fabian, A. C., & Blundell, K. M. 2008, MNRAS, 386, 1774
 Govoni, F., & Feretti, L. 2004, International Journal of Modern Physics D, 13, 1549
 Hardcastle, M. J. 2005, A&A, 434, 35
 Hardcastle, M. J., Birkinshaw, M. & Worrall, D. M., 2001, MNRAS, 323, L17
 Harris, D. E., & Grindlay, J. E. 1979, MNRAS, 188, 25
 Harris, D. E., & Grindlay, J. E. 1979, MNRAS, 188, 25
 Harris, D. E. & Krawczynski, H., 2002, ApJ, 565, 244
 Jamrozy, M., Konar, C., Machalski, J., & Saikia, D. J. 2008, MNRAS, 385, 1286
 Kaiser, C. R., Dennett-Thorpe, J., & Alexander, P. 1997, MNRAS, 292, 723
 Kataoka, J., Serino, J. P., Edwards, P. G., Kino, M., Takahara, F., Serino, Y., Kawai, N. & Martel, A. R., 2003, A&A, 410, 833
 Klamer, I. J., Ekers, R. D., Bryant, J. J., Hunstead, R. W., Sadler, E. M., & De Breuck, C. 2006, MNRAS, 371, 852
 Law-Green, J. D. B., Eales, S. A., Leahy, J. P., Rawlings, S. & Lacy, M., 1995, MNRAS, 277, 995
 Laing, R. A., & Peacock, J. A. 1980, MNRAS, 190, 903
 Landau, R., Golisch, B., Jones, T.J., Jones, T.W., Pedelty, J., Rudnick, L., Sitko, M., Kenney, J., Roelleg, T., Salonen, E., Urpo, S., Schmidt, G., Neugebauer, G., Matthews, K., Elias, J., Impey, C., Clegg, P., Harris, S. 1986, ApJ, 308, 78
 Longair, M.S., *High Energy Astrophysics*, C.U.P.
 McKinnon, M.M., Owen, F.N., & Eilek, J.A. 1991, ApJ, 101, 2026
 Miley, G. 1980, ARAA, 18, 165
 Mocz, P., Fabian, A.C., & Blundell, K.M. 2011, MNRAS, 413, 1107
 Rudnick, L., Katz-Stone, D. M., & Anderson, M. C. 1994, ApJS, 90, 955
 Scheuer, P. A. G. & Williams, P. J. S., 1968, ARAA, 6, 321
 Steenbrugge, K. C., Blundell, K. M., & Duffy, P. 2008, MNRAS, 388, 1465
 Sunyaev, R. A. & Zeldovich, Y. B., 1969, Nature, 223, 721

- Tucker, W. H. 1977, Radiation processes in astrophysics., by Tucker, W. H.. Cambridge, MA (USA): MIT Press
 Wardle, J. F. C., Homan, D. C., Ojha, R. & Roberts, D. H., 1998, Nature, 395, 457
 Wilson, A. S., Young, A. J. & Shopbell, P. L., 2001, ApJ, 547, 740
 Zeldovich, Y. B. & Sunyaev, R. A., 1970, ApSS, 7, 20

5 APPENDIX

The intrinsically-curved energy spectrum can be re-cast in terms of a log-normal distribution

$$\begin{aligned} N(\gamma) &= N_{\text{peak}} \exp \left[-q \left(\ln \left(\frac{\gamma}{\gamma_{\text{peak}}} \right) \right)^2 \right] \\ &= \frac{\hat{n}}{\sigma \sqrt{2\pi}} \frac{1}{\gamma} \exp \left[-\frac{(\ln \gamma - \mu)^2}{2\sigma^2} \right] \end{aligned} \quad (48)$$

using the substitutions,

$$\begin{aligned} \sigma &= \frac{1}{\sqrt{2q}} \\ \mu &= \frac{1}{2q} + \ln \gamma_{\text{peak}} \\ \hat{n} &= \sqrt{\frac{\pi}{q}} e^{1/4q} \gamma_{\text{peak}} N_{\text{peak}}. \end{aligned} \quad (49)$$

In probability theory if a random variable y has a Gaussian probability distribution, with mean μ and variance σ^2 , then its exponent, $x = e^y$, has a log-normal distribution (Aitchison & Brown 1957). With probability densities $P(x)$ and $P(y)$ this can be seen from the change of variable,

$$P(x) = P(y(x)) \left| \frac{dy}{dx} \right| = \frac{1}{\sigma \sqrt{2\pi}} \frac{1}{x} \exp \left[-\frac{(\ln x - \mu)^2}{2\sigma^2} \right] \quad (50)$$

where y takes on all values between $-\infty$ and ∞ while x lies between 0 and ∞ . That the energetic particle distribution in giant radio galaxy lobes has a shape close to the exponential of a normally-distributed variable is clearly saying something important about the physics involved in the acceleration process. For our current purposes we can exploit results on the first three moments of a log-normal function to derive useful approximations for the particle number density, energy density and total synchrotron power. The expectation value of x^m is given by

$$E[x^m] \equiv \int_0^\infty x^m P(x) dx = e^{m\mu + n^2 \sigma^2 / 2}. \quad (51)$$

We cannot apply this exact result to the log-normal form of the particle distribution function since $\gamma \geq 1$. However, we are interested in cases where on observational grounds, $\gamma_{\text{peak}} \gg 1$ and the number density is dominated by particles near that peak energy. For this reason, and also since we don't know a priori where any low energy cut-off might occur, the number density can be approximated by the zeroth moment ($m = 0$) of a log-normal distribution,

$$n = \frac{\hat{n}}{\sigma \sqrt{2\pi}} \int_1^\infty \frac{1}{\gamma} \exp \left[-\frac{(\ln \gamma - \mu)^2}{2\sigma^2} \right] d\gamma \approx \hat{n} E[\gamma^0] = \hat{n}. \quad (52)$$

The number density is therefore related to the peak properties and spectral curvature through

$$n = \sqrt{\frac{\pi}{q}} e^{1/4q} \gamma_{\text{peak}} N_{\text{peak}}. \quad (53)$$

For $m = 1$ and $m = 2$ we have

$$E[\gamma] = e^{3/4q} \gamma_{\text{peak}} \quad \text{and} \quad E[\gamma^2] = e^{2/q} \gamma_{\text{peak}}^2. \quad (54)$$

The particle energy density is then

$$U_{\text{P}} = nm_e c^2 E[\gamma] = \sqrt{\frac{\pi}{q}} e^{1/q} \gamma_{\text{peak}}^2 m_e c^2 N_{\text{peak}}, \quad (55)$$

and the second moment gives the total synchrotron luminosity in terms of peak properties and curvature,

$$\begin{aligned} P &= \frac{4}{3} \sigma_T c V U_{\text{B}} n E[\gamma^2] \\ &= \frac{4}{3} \sqrt{\frac{\pi}{q}} e^{9/4q} \sigma_T c V U_{\text{B}} \gamma_{\text{peak}}^3 N_{\text{peak}}. \end{aligned} \quad (56)$$

We make use of these relationships in Section 2.1.